

Phonon Transport in Suspended Single Layer Graphene

Xiangfan Xu^{1,2}, Yu Wang³, Kaiwen Zhang^{1,4}, Xiangming Zhao^{1,4}, Sukang Bae⁵,
Martin Heinrich⁶, Cong Tinh Bui⁶, Rongguo Xie^{1,4,7}, John T. L. Thong^{7,6},
Byung Hee Hong^{5,8}, Kian Ping Loh^{3,6}, Baowen Li^{1,4,6}, Barbaros Özyilmaz^{1,2,6*}

¹*Department of Physics, National University of Singapore, Singapore 117542*

²*NanoCore, 4 Engineering Drive 3, National University of Singapore, Singapore 117576*

³*Department of Chemistry, National University of Singapore, Singapore 117543*

⁴*Centre for Computational Science and Engineering,
National University of Singapore, Singapore 117542*

⁵*SKKU Advanced Institute of Nanotechnology (SAINT) and Center for Human Interface Nano Technology (HINT),
Sungkyunkwan University, Suwon 440-746, Korea*

⁶*NUS Graduate School for Integrative Science and Engineering, Singapore 117456*

⁷*Department of Electrical and Computer Engineering,
National University of Singapore, Singapore 117576 and*

⁸*Department of Chemistry, Sungkyunkwan University, Suwon 440-746, Korea*

(Dated: February 24, 2024)

We report the first temperature dependent phonon transport measurements in suspended Cu-CVD single layer graphene (SLG) from 15K to 380K using microfabricated suspended devices. The thermal conductance per unit cross section σ/A increases with temperature and exhibits a peak near $T \sim 280\text{K}$ ($\pm 10\text{K}$) due to the Umklapp process. At low temperatures ($T < 140\text{K}$), the temperature dependent thermal conductivity scales as $\sim T^{1.5}$, suggesting that the main contribution to thermal conductance arises from flexural acoustic (ZA) phonons in suspended SLG. The σ/A reaches a high value of $1.7 \times 10^5 T^{1.5} \text{ W/m}^2\text{K}$, which is approaching the expected ballistic phonon thermal conductance for two-dimensional graphene sheets. Our results not only clarify the ambiguity in the thermal conductance, but also demonstrate the potential of Cu-CVD graphene for heat related applications.

PACS numbers: 65.80.Ck, 63.22.Rc, 81.05.ue, 81.07.-b

Heat conduction in low-dimensional systems has been extensively studied in past decades because of its importance in understanding the microscopic mechanism of thermal transport phenomena, and its potential applications in manipulating and controlling heat flow [1]. Although significant progress has been made for one-dimensional systems [1], the study of heat conduction in two-dimensional (2D) systems is still in its infancy due to the lack of proper materials. The discovery of graphene has changed this scenario [2, 3]. It not only provides us with an ideal platform for thermal transport studies in 2D systems, but also opens the door for many novel heat related applications [4]. However, difficulties in integrating graphene sheets with device structures needed for measuring intrinsic thermal properties have resulted in experiments which only offer partial answers. Pioneering Raman based measurements at room temperature have indicated exceptional high thermal conductivity in graphene [5–7], far exceeding that of diamond [8] and carbon nanotubes [9, 10]. However, recent measurements have shown that these values can easily vary by one order of magnitude from 600 W/mK to 5300 W/mK [5, 11, 12]. Efforts to develop traditional suspended microfabricated heater wires have been only successful by compromising on the SiO_2 substrate, resulting in significant phonon leakage into the substrate and strong interfacial scattering between graphene and the underlying

substrate [13]. Therefore, the temperature dependent thermal conductivity $\kappa(T)$ needs to be investigated in suspended graphene. This will be the key in understanding the 2D nature of phonons in graphene and is crucial in identifying which phonon branch dominating the heat conduction.

In this Letter, we present the first temperature dependent thermal transport measurements in a suspended single layer graphene (SLG) sheet in the temperature range from 15K to 380K. Our approach takes advantage of the recent progress in wafer-scale graphene growth by the Cu-based chemical vapor deposition (Cu-CVD) method [14, 15]. The thermal conductivity follows a $T^{1.5}$ power law, demonstrating that most of the heat in free standing graphene is carried by flexural acoustic (ZA) phonons. At room temperature, the thermal conductance per unit cross section σ/A in Cu-CVD graphene reaches a high value of $3.8 \times 10^8 \text{ W/m}^2\text{K}$. Below 140K, this high value is found to be approaching the theoretical ballistic limit in graphene sheets [16, 17].

We employed typical prepatterned suspended heater wires to measure the thermal conductance and thermal power in suspended single layer graphene. Similar methods have been used to study thermal transport in carbon nanotubes [9, 18] and nanowire [19]. The structures were fabricated on silicon nitride (SiN_x)/Si multilayer wafers and the fabrication details have already been discussed

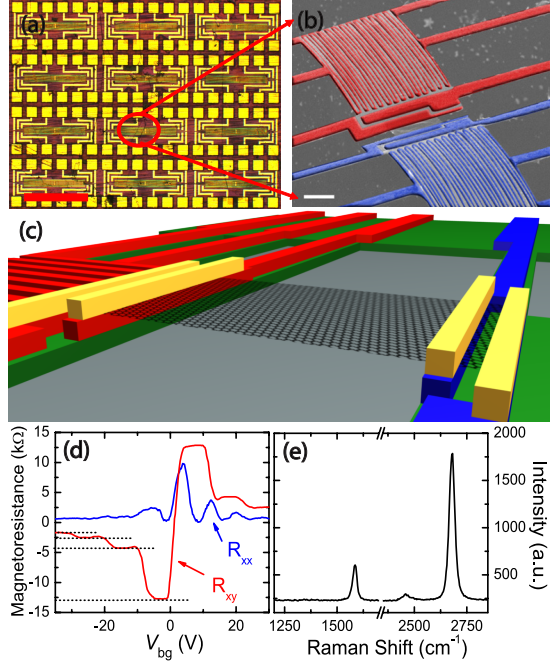


FIG. 1: (a) Microdevice array after CVD graphene transfer and before suspension. Only a 3×4 array section is shown, scale bar is 1mm. (b) False-color SEM image in the center of the suspended device. The red and blue Pt coils are the heater (R_h) and sensor (R_s), respectively. They are thermally connected by suspended graphene (grey rectangle in the middle). The inner four Pt electrodes are connected to graphene, but electrically isolated from Pt coils. The scale bar is $5 \mu\text{m}$. (c) Schematics of a graphene sheet clamped between Cr/Au (yellow) and Pt electrodes (blue and red) on SiN_x membranes (green). Lateral dimensions are not to scale. (d) Quantum Hall effect at $T=2\text{K}$, $B=9\text{T}$ and (e) Raman spectrum of the same batch of graphene transferred on regular Si/SiO₂ wafers.

by Shi *et al.* [20]. The transfer of exfoliated graphene onto such fragile structures is difficult and remains very challenging. Fortunately, the recent progress in Cu-CVD graphene allows us to overcome many of these challenges by the sheer number of available junctions on a single chip. The growth of SLG by Cu-CVD method is described elsewhere in detail [15]. The outstanding electronic properties and sub-100 micrometers grain size [21] suggest that the physical properties of Cu-CVD graphene are comparable to that of exfoliated graphene. Graphene films were transferred onto these prepatterned structures before suspending them (Figure 1a) [22]. They were then patterned into micrometer-size rectangular structures by standard e-beam lithography, followed by an O₂ plasma. In a second lithography step, 30nm Cr/Au bars were deposited on both ends of graphene to ensure good thermal contact with the Pt electrodes underneath graphene (Figure 1c). These Cr/Au bars also securely clamp graphene onto the Pt electrodes during the subsequent fabricating steps. After suspending graphene by etching in KOH, the

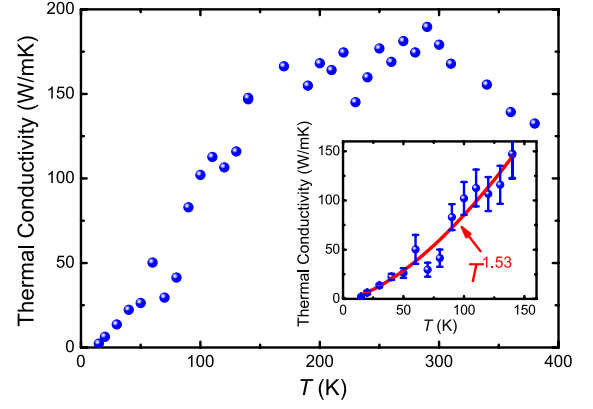


FIG. 2: Thermal conductivity κ versus temperature. Inset: thermal conductivity at low temperatures; the data can be fitted by $\kappa = bT^n$, where b is the fitting parameter and n is found to be $1.53(\pm 0.18)$.

devices were dried using a critical point dryer to avoid damage due to surface tension.

The scanning electron microscope image of a typical microfabricated device is shown in Figure 1b. The suspended device consists of two $25 \times 20 \mu\text{m}^2$ SiN_x membranes, each of which is supported by six $400 \mu\text{m}$ -long, $0.3 \mu\text{m}$ -thick and $1.5 \mu\text{m}$ -wide suspended SiN_x beams. A 60nm -thick platinum resistor coil is deposited on top of each SiN_x membrane. Since the resistance of the Pt resistors changes with temperature, they can serve as both heater (R_h) and temperature sensor (R_s). The suspended graphene (grey sheet in the middle of Figure 1b) bridges the two SiN_x membranes and is electrically isolated from the Pt coils. In total, three samples from two separate Cu-CVD growth runs have been measured. Here we discuss representative data based on one graphene sheet, which is patterned to a width of $3 \mu\text{m}$ and a suspended length of 500nm . Since there is no back gate for such suspended graphene samples (etch depth $\approx 200 \mu\text{m}$), we could neither vary the carrier density nor calculate the mobility. However, this is not a severe limitation in our measurements due to the following reasons: a) thermal conductance in graphene is weakly dependent on carrier density; b) we can set the Fermi level near Dirac point by *in-situ* annealing in vacuum [23]; c) the sample quality can be investigated by characterizing the same batch of graphene on SiO₂. The measured mobility is approximately $7700\text{cm}^2/\text{Vs}$ at $T=2\text{K}$, which is comparable to that in exfoliated graphene. The half-integer quantum Hall measurements at $T=2\text{K}$ and $B=9\text{T}$ (Figure 1d) and Raman measurements (Figure 1e) also indicate high quality of our graphene samples.

We now turn to the experimental results and discuss first the temperature dependent thermal conductivity $\kappa(T)$. Figure 2 shows the thermal conductivity κ in the temperature range from 15K to 380K of the suspended

sample G1. κ is extracted from $\kappa = \sigma L/A$, where L is the sample length, A is the cross section area of graphene and σ is the measured thermal conductance of graphene [22]. The observed κ increases by two orders of magnitude as the temperature increases, reaches a maximum of 190 W/mK at $T \sim 280\text{K} (\pm 10\text{K})$ and decreases at higher temperature. The most important result is the low temperature behavior of κ . The inset of Figure 2 shows that κ can be fitted by $\kappa = bT^n$. Here, b is the fitting parameter and n is found to be $1.53(\pm 0.18)$. Theoretical work has predicted that the thermal conductivity in graphene yields a power law of $\sim T^n$, where n varies from 1 for one-dimensional nanoribbons to 1.5 for two-dimensional graphene sheets [17]. It is worth noting that this $T^{1.5}$ power law at low temperatures was not observed in supported graphene [13]. Our measurements of the $T^{1.5}$ law directly reveals for the first time unambiguously intrinsic phonon transport in graphene sheets.

We shall now interpret the physics behind the observed $\kappa(T)$. The acoustic vibrations in 2D graphene lattice are composed of two types of phonons: in-plane phonons (TA and LA phonons) with linear dispersion, and out-of-plane phonons (ZA phonons or flexural acoustic phonons) with quadratic dispersion. It was proposed that only in-plane acoustic phonons carry heat in graphene and the contribution from out-of-plane phonons can be neglected [24]. This arises from the fact that the group velocity of ZA phonons is approaching zero for wave vector, $\mathbf{q} \rightarrow 0$. However, Mingo *et al.* have argued that the ZA phonons carry most of the heat in SLG [25]. This is due to the large density of modes for ZA phonons resulting from their quadratic dispersion. At low temperatures, the in-plane LA and TA modes would introduce a $\sim T^2$ contribution to the thermal conductivity, while the contribution from ZA mode scales as $\sim T^{1.5}$ [16, 17]. The observed $\sim T^{1.5}$ behavior therefore proves that the thermal conductivity in suspended SLG mainly arises from ZA phonons.

Interestingly, even before the first exfoliation of graphene, Klemens [26] had predicted that low-frequency phonon leakage into the substrate will reduce thermal conductivity by 20% to 50%. Therefore, the measured $\kappa(T)$ in this work is much closer to the intrinsic phonon transport than that measured in supported graphene. The observed $T^{1.5}$ behavior is different from that of supported graphene and suggests that ZA phonons carry most of the heat in suspended SLG. Theoretical calculations also show that ZA phonons contribute more than 75% to κ in suspended graphene below room temperature [25], which is consistent with our results. The same power law is also observed in samples with much inferior quality, suggesting that this $T^{1.5}$ behavior is not strongly dependent on the quality of the samples and may be intrinsic to phonon transport in 2D systems (See Supplementary Information).

As the temperature increases further, the strong phonon-phonon Umklapp scattering becomes more effective

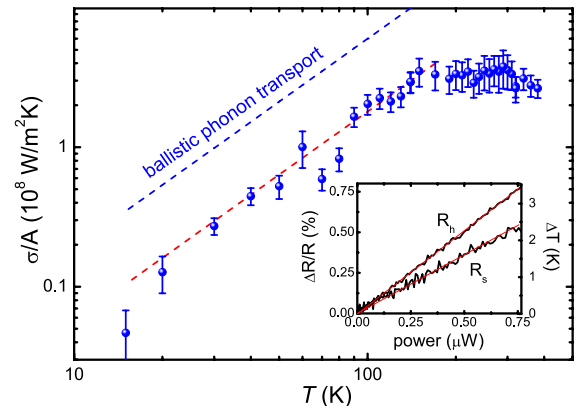


FIG. 3: Thermal conductance per unit cross section σ/A of sample G1 as a function of temperature (solid circles). The data can be fitted by $1.7 \times 10^5 T^{1.53}$ W/m²K (red dashed curve). The measured data is approaching the expected ballistic limit in graphene sheets (blue dashed curve). Inset: the temperature and resistance changes in the heater resistor R_h and sensor resistor R_s as a function of applied Joule heat, the red lines are guides to the eye.

and dominates the thermal conductivity due to thermally excited higher energy phonons. It leads to a deviation from the $\sim T^{1.5}$ law and a maximum in thermal conductivity around $\sim 280\text{K} (\pm 10\text{K})$, followed by a decrease with a further increase of temperature. This peak in thermal conductivity near room temperature is consistent with experimental reports in supported graphene [13, 27] and carbon nanotubes [9]. At low temperatures where the phonon-phonon Umklapp scattering is suppressed, phonon transport will approach the ballistic limit if the graphene sheet is clean enough.

Next, we discuss the thermal conductance per unit cross section σ/A as a function of temperature. At room temperature σ/A is 3.8×10^8 W/m²K (Figure 3). This value is comparable to the values observed in suspended exfoliated SLG samples based on Raman measurements ($3\text{--}5 \times 10^8$ W/m²K) [5, 7]. The high quality of CVD graphene is further confirmed by the temperature dependence of σ/A . It decreases by a factor of 100 to approximately 4.5×10^6 W/m²K at 15 K. Such a steep decrease has not been observed previously, but more interestingly, the data at low temperatures can be fitted with $1.7 \times 10^5 T^{1.53}$ W/m²K. This is shown as the dashed red curve in Figure 3 and has important implications for the nature of phonon transport. Mingo and Brodio proposed that for ballistic phonon transport, σ/A follows $6 \times 10^5 T^{1.5}$ W/m²K [16], as shown by the blue dashed curve in the same figure. The experimentally observed value is close to 30% of the predicted ballistic thermal conductance for graphene. From this we conclude that in our sample with a channel length of 500nm phonon transport approaches the ballistic limit. It is important to note that even in multiwalled CNT, the experimentally

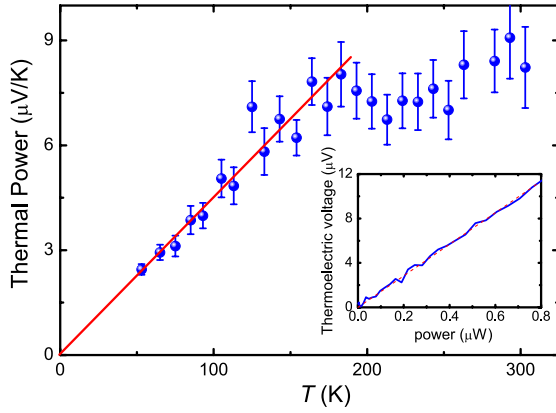


FIG. 4: The measured thermoelectric power (solid circles) and a linear fit (red curve) for $T < 180\text{K}$. Inset: the thermoelectric voltage as a function of applied Joule heat, the red dashed line is a guide to the eye.

observed σ/A reached at most 40% of the ballistic limit in graphite [9, 16]. Deviation from ballistic transport in our experiment is most likely caused by scattering from PMMA residues, CVD graphene specific organic contamination, ripples and CVD graphene specific defects [28] such as wrinkles. However, even in the absence of defects and contamination, two additional source remain: a) scattering from naturally existing 1.1% ^{13}C isotopic impurities [29] and b) scattering from the boundaries between the suspended area and the supported areas on top of the contacts.

Last but not least, we discuss the thermoelectric power (TEP) of suspended graphene samples. Shown in the inset of Figure 4 is the linear thermoelectric voltage as a function of Joule heat in R_h (blue curve). Since TEP and its temperature dependence vary sharply across the Dirac point and we do not have a gate control, a direct comparison with supported samples is difficult. At room temperature the observed value is $+9\text{ }\mu\text{V/K}$, suggesting a hole-like majority carrier. The linear fit (red curve in Figure 4) to our data can be extrapolated to zero at $T=0\text{K}$. Similar to TEP measurements in supported graphene [30], this confirms the absence of phonon drag in suspended CVD SLG.

In conclusion we have measured phonon transport in suspended graphene as a function of temperature from 380 K down to 15K. We have taken advantage of the recent progress in Cu based CVD graphene and observed a $T^{1.5}$ power in these samples. Our results clearly show that the thermal conductance is strongly dominated by ZA phonons. At low temperatures phonon transport is approaching the ballistic limit, demonstrating the high quality of CVD graphene samples also in the context of heat transport.

We thank Y. Zheng for helping with measurements

and C.T. Toh for helping with fabrication. This work is supported in part by Singapore National Research Foundation (NRF-RF2008-07), NRF-CRP grant (R-143-000-360-281), by a NUS grant (R-144-000-222-646), by A*STAR grant (R-143-000-360-311), and by NUS NanoCore.

* Electronic address: barbaros@nus.edu.sg

- [1] A. Dhar, Adv. Phys. **57**, 457 (2008); L. Wang and B. Li, Phys. World **21**, 27 (2008).
- [2] K.S. Novoselov *et al.*, Science **306**, 666 (2004); K.S. Novoselov *et al.*, Nature **438**, 197 (2005); Y.B. Zhang, Y.W. Tan, H.L. Stormer and P. Kim, Nature **438**, 201 (2005).
- [3] A.H. Castro Neto *et al.*, Rev. Mod. Phys. **81**, 109 (2009).
- [4] E. Pop, Nano Res. **3**, 147 (2010).
- [5] A.A. Balandin *et al.*, Nano Lett. **8**, 902 (2008).
- [6] S. Ghosh *et al.*, Appl. Phys. Lett. **92**, 151911 (2008).
- [7] S. Ghosh *et al.*, Nat. Mater. **9**, 555 (2010).
- [8] L. Wei *et al.*, Phys. Rev. Lett. **70**, 3764 (1993).
- [9] P. Kim, L. Shi, A. Majumdar and P.L. McEuen, Phys. Rev. Lett. **87**, 215502 (2001).
- [10] E. Pop *et al.*, Nano Lett. **6**, 96 (2006).
- [11] C. Faugeras *et al.*, Acs Nano **4**, 1889 (2010).
- [12] W.W. Cai *et al.*, Nano Lett. **10**, 1645 (2010).
- [13] J.H. Seol *et al.*, Science **328**, 213 (2010).
- [14] X.S. Li *et al.*, Science **324**, 1312 (2009).
- [15] S. Bae *et al.*, Nat. Nanotechnol. **5**, 574 (2010).
- [16] N. Mingo and D.A. Broido, Phys. Rev. Lett. **95**, 096105 (2005).
- [17] E. Muñoz, J.X. Lu and B.I. Yakobson, Nano Lett. **10**, 1652 (2010).
- [18] C.W. Chang, D. Okawa, A. Majumdar and A. Zettl, Science **314**, 1121 (2006).
- [19] R.K. Chen *et al.*, Phys. Rev. Lett. **101**, 105501 (2008); A.I. Hochbaum *et al.*, Nature **451**, 163 (2008).
- [20] L. Shi *et al.*, J. Heat Transfer **125**, 881 (2003).
- [21] The grain size of CVD SLGs is in the order of $20\mu\text{m} \times 20\mu\text{m}$, while the devices for the thermal measurements have lateral dimensions of $\approx 3\mu\text{m} \times 1\mu\text{m}$. Hence, the samples have, if at all only one grain boundary at most.
- [22] please refer to the supplementary information for details.
- [23] X. Du, I. Skachko, A. Barker and E.Y. Andrei, Nat. Nanotechnol. **3**, 491 (2008).
- [24] D.L. Nika, E.P. Pokatilov, A.S. Askerov and A.A. Balandin, Phys. Rev. B **79**, 155413 (2009).
- [25] L. Lindsay, D.A. Broido and N. Mingo, Phys. Rev. B **82**, 115427 (2010).
- [26] P.G. Klemens, Int. J. Thermophys., **22**, 265 (2001).
- [27] W.Y. Jang *et al.*, Nano Lett. **10**, 3909 (2010).
- [28] O.V. Yazyev and S.G. Louie, Nat. Mater. **9**, 806 (2010).
- [29] J.W. Jiang, J.H. Lan, J.S. Wang and B. Li, J. Appl. Phys. **107**, 054314 (2010).
- [30] Y.M. Zuev, W. Chang and P. Kim, Phys. Rev. Lett. **102**, 096807 (2009); J.G. Checkelsky and N.P. Ong, Phys. Rev. B **80**, 081413(R) (2009).